

AD-A225 784

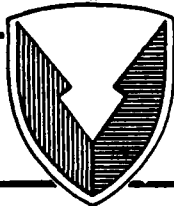
TECHNICAL REPORT RD-DE-90-2



**A PERFORMANCE ANALYSIS AND CHARACTERIZATION OF THE LUMONICS INC. HYPERDYE-300 LASER PUMPED DYE LASER**

Travis S. Taylor  
Wayne E. Davenport  
John J. Ehrlich  
Directed Energy Directorate  
Research, Development, and Engineering  
Center

JULY 1990



**U.S. ARMY MISSILE COMMAND**

*Redstone Arsenal, Alabama* 35898-5000

*Cleared for public release; distribution is unlimited.*

DTIC  
ELECTE  
AUG 28 1990  
S B D  
Co

### DESTRUCTION NOTICE

FOR CLASSIFIED DOCUMENTS, FOLLOW THE PROCEDURES IN DoD 5200.22-M, INDUSTRIAL SECURITY MANUAL, SECTION II-19 OR DoD 5200.1-R, INFORMATION SECURITY PROGRAM REGULATION, CHAPTER IX. FOR UNCLASSIFIED, LIMITED DOCUMENTS, DESTROY BY ANY METHOD THAT WILL PREVENT DISCLOSURE OF CONTENTS OR RECONSTRUCTION OF THE DOCUMENT.

### DISCLAIMER

THE FINDINGS IN THIS REPORT ARE NOT TO BE CONSTRUED AS AN OFFICIAL DEPARTMENT OF THE ARMY POSITION UNLESS SO DESIGNATED BY OTHER AUTHORIZED DOCUMENTS.

### TRADE NAMES

USE OF TRADE NAMES OR MANUFACTURERS IN THIS REPORT DOES NOT CONSTITUTE AN OFFICIAL ENDORSEMENT OR APPROVAL OF THE USE OF SUCH COMMERCIAL HARDWARE OR SOFTWARE.

UNCLASSIFIED

SECURITY CLASSIFICATION OF THIS PAGE

REPORT DOCUMENTATION PAGE				Form Approved OMB No. 0704-0188	
1a. REPORT SECURITY CLASSIFICATION UNCLASSIFIED		1b. RESTRICTIVE MARKINGS			
2a. SECURITY CLASSIFICATION AUTHORITY		3. DISTRIBUTION / AVAILABILITY OF REPORT			
2b. DECLASSIFICATION / DOWNGRADING SCHEDULE		Cleared for public release; distribution is unlimited			
4. PERFORMING ORGANIZATION REPORT NUMBER(S) TR-RD-DE-90-2		5. MONITORING ORGANIZATION REPORT NUMBER(S)			
6a. NAME OF PERFORMING ORGANIZATION Directed Energy Directorate RD&E Center		6b. OFFICE SYMBOL (if applicable) AMSMI-RD-DE	7a. NAME OF MONITORING ORGANIZATION		
6c. ADDRESS (City, State, and ZIP Code) Redstone Arsenal, AL 35898		7b. ADDRESS (City, State, and ZIP Code)			
8a. NAME OF FUNDING / SPONSORING ORGANIZATION	8b. OFFICE SYMBOL (if applicable)	9. PROCUREMENT INSTRUMENT IDENTIFICATION NUMBER			
8c. ADDRESS (City, State, and ZIP Code)		10. SOURCE OF FUNDING NUMBERS			
		PROGRAM ELEMENT NO.	PROJECT NO.	TASK NO.	WORK UNIT ACCESSION NO.
11. TITLE (Include Security Classification) A PERFORMANCE ANALYSIS AND CHARACTERIZATION OF THE LUMONICS, INC. HYPERDYE-300 LASER PUMPED DYE LASER					
12. PERSONAL AUTHOR(S) Travis S. Taylor, Wayne E. Davenport, John J. Ehrlich					
13a. TYPE OF REPORT Final		13b. TIME COVERED FROM _____ TO _____	14. DATE OF REPORT (Year, Month, Day) 1990/July/11		15. PAGE COUNT 32
16. SUPPLEMENTARY NOTATION					
17. COSATI CODES			18. SUBJECT TERMS (Continue on reverse if necessary and identify by block number)		
FIELD	GROUP	SUB-GROUP	Nd:YAG Pumped Dye Laser HyperDYE-300 Dye Laser		
19. ABSTRACT (Continue on reverse if necessary and identify by block number) The laser analyzed in this research, the Lumonics, Inc. HyperDYE-300 laser pumped dye laser, was procured via the FSTC D650 Program and was characterized in order to support the technology development of that program. The dye laser was pumped with a Neodymium:YAG q-switched laser and it utilized Rhodamine-6G in methanol. It was found to be tunable from about 545 nm to 590 nm and produced a maximum output energy of 56 percent of the pump beam energy. The analysis involved the measuring of optimum dye/solvent concentration, output energy versus tunability, optical efficiency versus tunability, temporal and spatial profiles, beam divergence, linewidth, and amplified spontaneous emission versus laser emission.					
20. DISTRIBUTION / AVAILABILITY OF ABSTRACT <input type="checkbox"/> UNCLASSIFIED/UNLIMITED <input checked="" type="checkbox"/> SAME AS RPT <input type="checkbox"/> DTIC USERS			21. ABSTRACT SECURITY CLASSIFICATION UNCLASSIFIED		
22a. NAME OF RESPONSIBLE INDIVIDUAL Travis S. Taylor		22b. TELEPHONE (Include Area Code) 205-876-8182		22c. OFFICE SYMBOL AMSMI-RD-DE-LT	

DD Form 1473, JUN 86

Previous editions are obsolete.

SECURITY CLASSIFICATION OF THIS PAGE  
UNCLASSIFIED

### ACKNOWLEDGEMENTS

The authors would like to acknowledge the following people for the various types of assistance that they offered throughout this research. Most importantly, appreciation goes to the FSTC D650 program, which enabled the procurement of the dye laser utilized in this research. Certain aspects of the characterization of this dye laser were investigated by a SEAP apprentice, Mr. Lorne Graves, and his mentor, Mr. Bill Mullins, both of whom offered consultation concerning the alignment procedures and output energy versus tunability measurements for this dye laser. Mr. Bill Friday also offered technical consultation as well as helping with the abstract of this report. Finally, the authors would like to acknowledge Dr. Frank J. Duarte for the assistance he offered with the ASE measurements and the linewidth calculations.

<b>Accession For</b>	
NTIS GRA&I	<input checked="" type="checkbox"/>
DTIC TAB	<input type="checkbox"/>
Unannounced	<input type="checkbox"/>
Justification	
By	
Distribution/	
Availability Codes	
Dist	Avail and/or Special
A-1	



CONTENTS

	<u>Page</u>
I. INTRODUCTION.....	1
II. HYPERDYE-300 SERIES DESIGN CONCEPT.....	2
III. ALIGNMENT AND OPTIMIZATION OF EXPERIMENTAL SETUP.....	4
IV. DATA.....	10
V. CONCLUSIONS.....	24
REFERENCES.....	25

LIST OF ILLUSTRATIONS

<u>Figure</u>	<u>Title</u>	<u>Page</u>
1.	Optical cavity for Nd:YAG pump beam and the HyperDYE-300 dye laser.....	3
2.	Flourescence and absorption curves of R-6G in MeOH.....	5
3.	Fabry-Perot rings of dye laser output.....	7
4.	Fabry-Perot rings of broad bandwidth ASE.....	7
5.	Fabry-Perot rings of narrow linewidth dye laser output.....	7
6.	Dye laser output energy vs dye concentration.....	8
7.	Dye laser output energy vs wavelength.....	11
8.	Optical efficiency vs wavelength.....	12
9.	Energy of HyperDYE-300 output vs energy of Nd:YAG output.....	13
10.	Slope efficiency of HyperDYE-300.....	14
11.	Temporal profile of Nd:YAG output.....	15
12.	Temporal profile of HyperDYE-300 output.....	15
13.	Single mode temporal profile of HyperDYE-300 output.....	15
14.	Spatial profile of low energy dye laser pulse.....	16
15.	Spatial profile of high energy dye laser pulse.....	17
16.	Spectral purity of HyperDYE-300 oscillator.....	20
17.	Spectral purity of HyperDYE-300 oscillator.....	21
18.	Spectral purity of HyperDYE-300 oscillator-amplifier.....	22

## I. INTRODUCTION

This report is an analysis and characterization of the Lumonics, Inc. HyperDYE-300 laser pumped dye laser, which was chosen for acquisition through the FSTC D650 program. The dye laser was utilized in this research as a Neodymium:YAG pulsed laser pumped dye laser. The performance of the dye laser was optimized and then several aspects of its performance were characterized. This included: dye/solvent concentration versus output energy, output energy versus wavelength, optical efficiency versus wavelength, temporal profiles, and spatial profiles.

Linewidth was also measured and compared to the theoretical linewidth for this type of laser. Along with the linewidth, the amount of amplified spontaneous emission (ASE) created within the dye laser cavity, which is a problem with many laser pumped dye lasers, was measured. Linewidth and ASE are closely related to one another. If there is a large amount of ASE in a laser cavity, then the linewidth of the laser output typically will not be optimized. Methods to decrease the amount of ASE in the HyperDYE-300 were investigated and implemented in order to decrease the linewidth.

The Hyper DYE-300 utilizes a hybrid multi-prism grazing-incidence type oscillator and a high gain amplifier. This type of laser cavity is known for being tunable, having a narrow linewidth, and having good beam quality. The performance analysis of this dye laser was done in order to determine if the HyperDYE-300 does indeed exhibit characteristics indigenous to this type of dye laser.

## II. HYPERDYE-300 SERIES DESIGN CONCEPT

The HyperDYE-300 series of pulsed dye lasers from Lumonics, Inc. were, according to the manufacturer, designed to be a simple and versatile tool for applications where a source of laser light is needed. The laser was designed to utilize various pump sources ranging from excimer lasers to frequency doubled and tripled Neodymium:YAG (Nd:YAG) lasers. The HyperDYE-300 consists of a tunable oscillator, an amplifier, and the necessary pump beam steering optics. Due to the oscillator design, the dye laser allows rapid alignment and simple operation. The oscillator is of a design that has a fairly narrow linewidth and still maintains good energy conversion efficiency.

The oscillator is a hybrid multi-prism grazing-incidence cavity. Most grazing-incidence cavities require an angle of incidence of approximately 89 degrees. An angle of incidence this large causes the laser cavity to be very inefficient. However, this inefficiency can be overcome by utilizing a beam expander. In the HyperDYE-300 (see Fig. 1) an achromatic, four-prism beam expander (PBE) is placed between the oscillator dye cell and a holographic grating (GR1). The 15X four-prism beam expander in the HyperDYE-300 expands the beam enough so that the angle of incidence can be decreased to 85 degrees. This smaller incidence angle is much better for efficient laser operation. The beam expander and grating are always in a fixed position so that the laser beam is always illuminating the same number of lines on the grating. This insures that there is no change in linewidth due to a change in lasing wavelength, since the wavelength is changed by adjusting the 100 percent reflector (M7) instead of the grating.

The reflector (M7) is mounted on a rotary drive stage (or stepper motor) that has an optical encoder. The optical encoder records the mirror angle and is translated via microelectronic devices into wavelength. The microelectronics are part of a SCAN unit which is used to control the tuning mirror angle and the rate at which it can be changed. The unit is easily calibrated so that the electronics displays the lasing wavelength to within a hundredth of a nanometer.

The HyperDYE-300 is equipped with a 2400 lines/mm holographic grating which is appropriate for laser operation at wavelengths from 320 to 730 nm. The grating is factory mounted and prealigned on a kinematic mount so oscillator alignment is not necessary by the user. The grating is also mounted in the oscillator with a skew in its axis. This prevents the grating and the tuning mirror from ever being parallel to one another, which in cases where there is enough gain, two lines begin to lase. The built-in skew of the grating axis is sufficient to prevent this from happening without interfering with the tuning capabilities of the cavity.

The oscillator output passes through a broadband partially reflecting output coupler (M6) and into a beam expanding telescope (BET). The BET consists of two lenses, a diverging lens (L3) and a collimating lens (L4). The oscillator beam is expanded in order to fill as much as possible of the amplifier gain volume. The BET also helps reduce the divergence of the output laser beam.



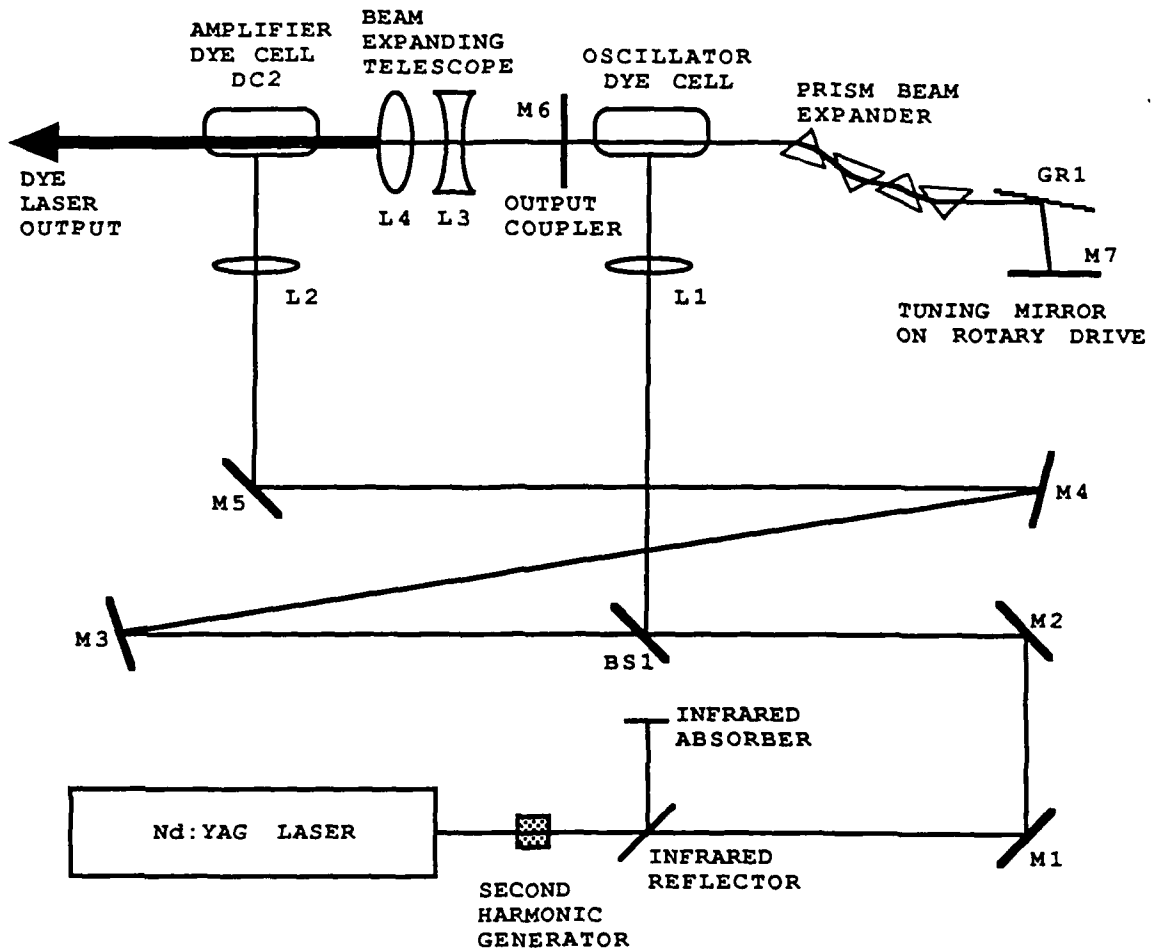


Figure 1. Optical cavity for the Nd:YAG pump beam and the HyperDYE-300 dye laser.

### III. ALIGNMENT AND OPTIMIZATION OF EXPERIMENTAL SETUP

In this research a Nd:YAG laser was used as the pump source. Nd:YAG typically lases at a wavelength of 1064 nm and when this is frequency doubled or tripled, it is an excellent pump source for pumping visible dye lasers. The decision was made to use doubled Nd:YAG (532 nm laser wavelength) as the pump source. The reasoning behind this decision can be seen in Figure 2 which shows the absorption and fluorescence curves for Rhodamine-6G (R-6G) in methanol solvent. From this figure it can be seen that R-6G absorbs light at a wavelength of 532 nm very well. This means that doubled Nd:YAG is a very good pump source for R-6G. As it turned out, the peak lasing wavelength for the HyperDYE-300 was 566 nm, which is where the absorption curve stops and is high on the fluorescence curve. This data is typical of doubled Nd:YAG pumped R-6G.

Figure 1 is a schematic of the optical assembly. The 1064 nm output of the Nd:YAG was passed through a second harmonic generator where the majority of the output becomes 532 nm. The beam was then passed through a dichroic beam splitter that reflects 1064 nm and transmits 532 nm. This removes all of the unwanted 1064 nm photons from the pump beam. The 532 nm beam was then reflected off of two turning mirrors (M1 and M2) to aid in the aligning of the pump beam properly into the dye laser. Once the Nd:YAG beam is aligned straight into the dye laser, it is split by a beam splitter (BS1) into two components. Ten percent of the beam is reflected onto a cylindrical lens (L1) and is then focused onto the dye cell of the oscillator (DC1). The remaining ninety percent of the pump beam is delayed by reflecting off three mirrors (M3, M4, and M5). The pump beam is reflected from M5 onto a cylindrical lens (L2) which then focuses the pump beam onto the amplifier dye cell (DC2).

Since the oscillator cavity is aligned by the manufacturer, the only alignment procedure required here is to focus the pump beam onto the dye cell and to use the SCAN unit to tune the tuning mirror until the brightest laser spot appears. The BET is then aligned using the targets supplied by the manufacturer. To aid in alignment procedures there is a knife blade in the amplifier cell. As the expanded oscillator beam passes through the amplifier a shadow of the knife-edge appears. Proper alignment procedure is to focus the brightest part of the oscillator beam approximately one millimeter below the knife-edge.<sup>1</sup>

The HyperDYE-300 pulsed dye laser was designed to allow only ten percent of the pump beam to pump the oscillator while the other ninety percent is delayed and then utilized to pump the single pass amplifier. Obviously, most of the gain occurs in the amplifier.

Since there is such a large amount of gain in the amplifier, amplified spontaneous emission (ASE) is a problem. Although the HyperDYE-300 was designed with pump beam delays that only allow the amplifier to "turn-on" after the oscillator has begun lasing, parasitic ASE takes place due to reflections off of the lenses in the BET. However, by offsetting the BET with respect to the amplifier cell, the parasitic ASE was diminished slightly. Of course, other ASE paths did occur due to reflections off of the dye cell windows; however, only the ASE that was in the single pass pathway of the

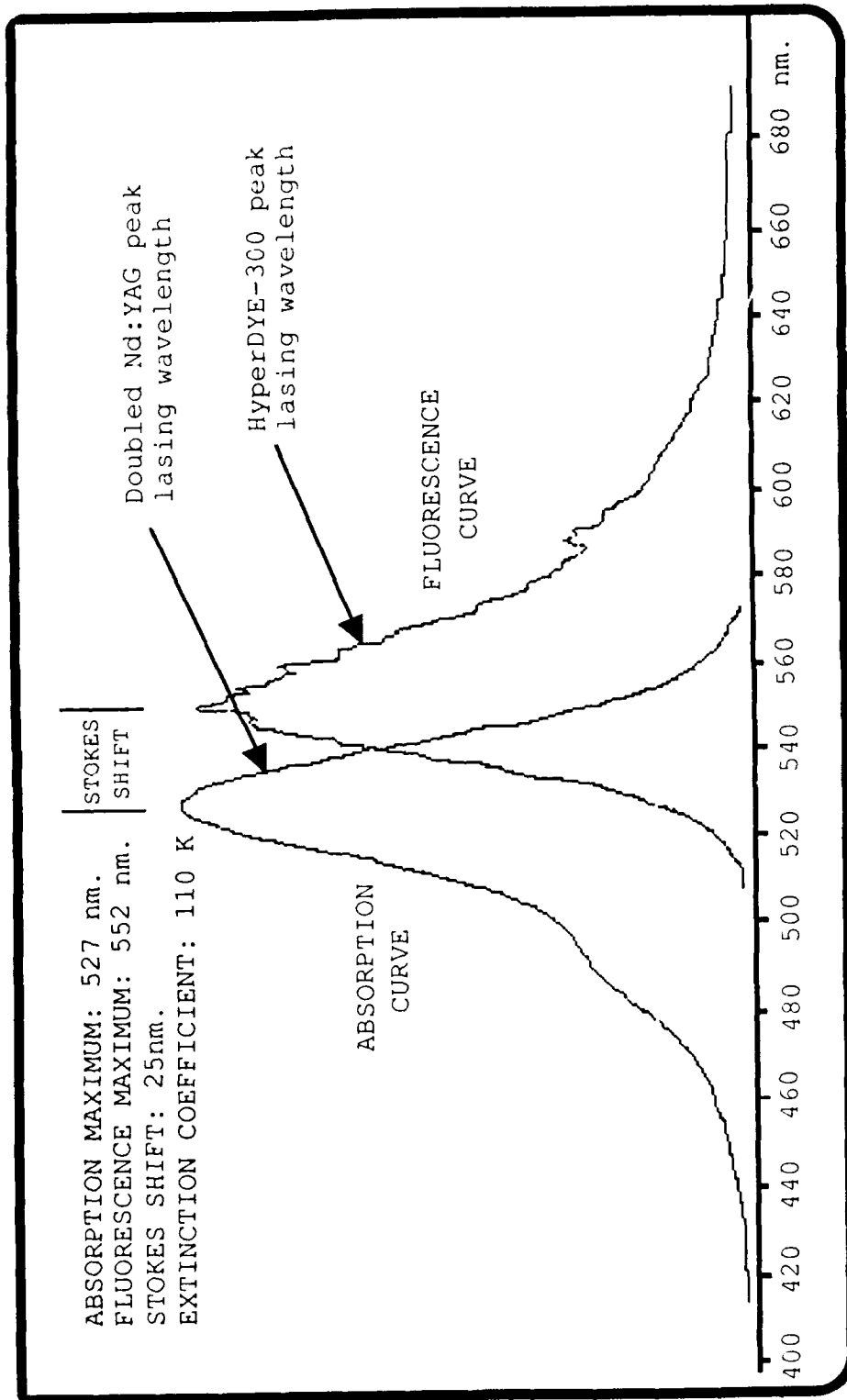


Figure 2. Fluorescence and absorption curves of Rhodamine-6G in MeOH.

oscillator-amplifier was of concern. Other ASE paths were removed with an aperture. Unfortunately, all of the ASE was not defeated in this manner.

Figure 3 shows the dye laser output when passed through a Fabry-Perot interferometer. Note that the ring pattern suggests that there were two lines lasing at the same time. One line was due to the oscillator-amplifier pathway, while the other was caused by ASE in the amplifier. Apparently, the gain in the amplifier dye cell was enough to cause problems even with the BET offset. Figure 4 is a picture of the ring pattern produced by passing the amplifier ASE through the Fabry-Perot while the oscillator was blocked. These rings reveal the broadband emissions that would be expected by ASE. The only way to suppress this ASE was by decreasing the energy per area of the amplifier pump beam. This was done by defocusing the cylindrical lens (L2) until the fringes created by the ASE disappeared.

Figure 5 displays the type of output that was finally achieved with the oscillator-amplifier. Note that the rings are only in bright solid bands which suggests only one line of laser operation. Hence, the ASE was suppressed by defocusing the pump beam; however, the output energy of the laser beam decreased as well. This is to be expected since the pump energy per area was decreased. It should be mentioned that the optics in the dye laser are not anti-reflection coated which is why there is such an ASE problem to begin with. If the optics were anti-reflection coated, then perhaps the BET could be aligned properly and the amplifier pump beam could be focused onto the dye cell properly. This would most certainly increase the output energy a considerable amount and ASE might not be such a problem.

The concentration of the dye was also found to be a factor in controlling the ASE of the HyperDYE-300. Utilizing the dye Rhodamine-6G (R-6G), it was observed that with too high a concentration the amplifier cell would "lase" on its own cell windows. In order to find the optimum concentration to use in the dye laser, its .5 liter reservoir was first filled with pure methanol and then one milliliter increments of  $1.25 \times 10^{-3}$  Molar R-6G in methanol was added to the dye reservoir. Figure 6 displays the dye laser output energy versus the dye concentration. The dye laser did not lase until the concentration was at least  $2.5 \times 10^{-5}$  Molar and its output energy did not increase noticeably until the concentration was about  $5 \times 10^{-5}$  Molar. At a concentration of approximately  $9.75 \times 10^{-5}$  the amplifier cell began to lase off of its windows. However, as stated before, the ASE pathways were not within the oscillator-amplifier axis, so at this concentration ASE was not parasitic to the dye laser output. As the concentration increased, the output energy obviously increased, unfortunately, the ASE increased as well. The optimum output concentration was found to be  $1.5 \times 10^{-4}$  Molar. At concentrations slightly higher than this the ASE began to affect the lasing pathway by a noticeable amount.

Since the HyperDYE-300 only has one dye reservoir, the same dye flows through both the oscillator and the amplifier. It is quite possible that two separate dye reservoirs - one for the oscillator and one for the amplifier - would be beneficial. The design of the oscillator limits the ASE that can occur there, but the ASE in the amplifier is mostly a function of the concentration. The higher the concentration of the dye in the amplifier

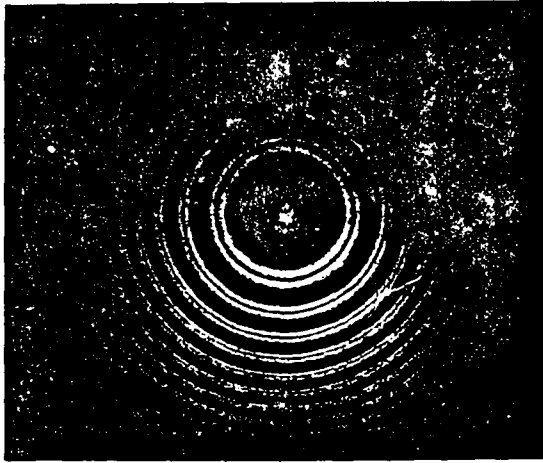


Figure 3. Fabry-Perot rings of the dye laser output shows two different lines "lasing".

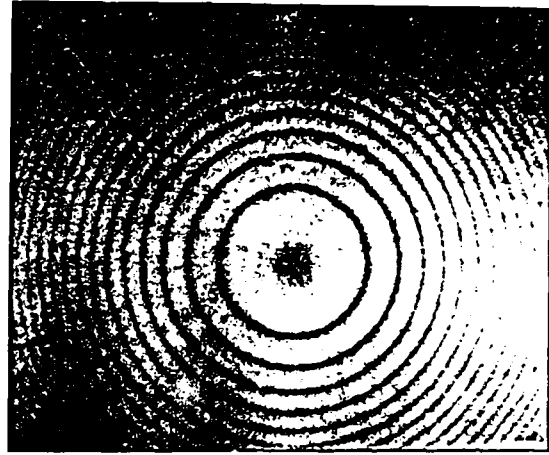


Figure 4. Fabry-Perot rings of broad bandwidth ASE.

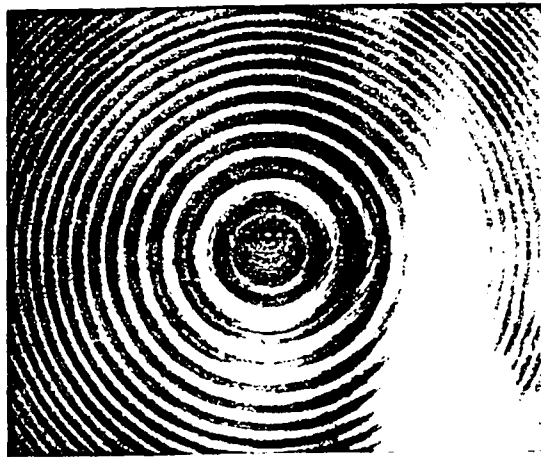


Figure 5. Fabry-Perot rings of the narrow linewidth dye laser output.

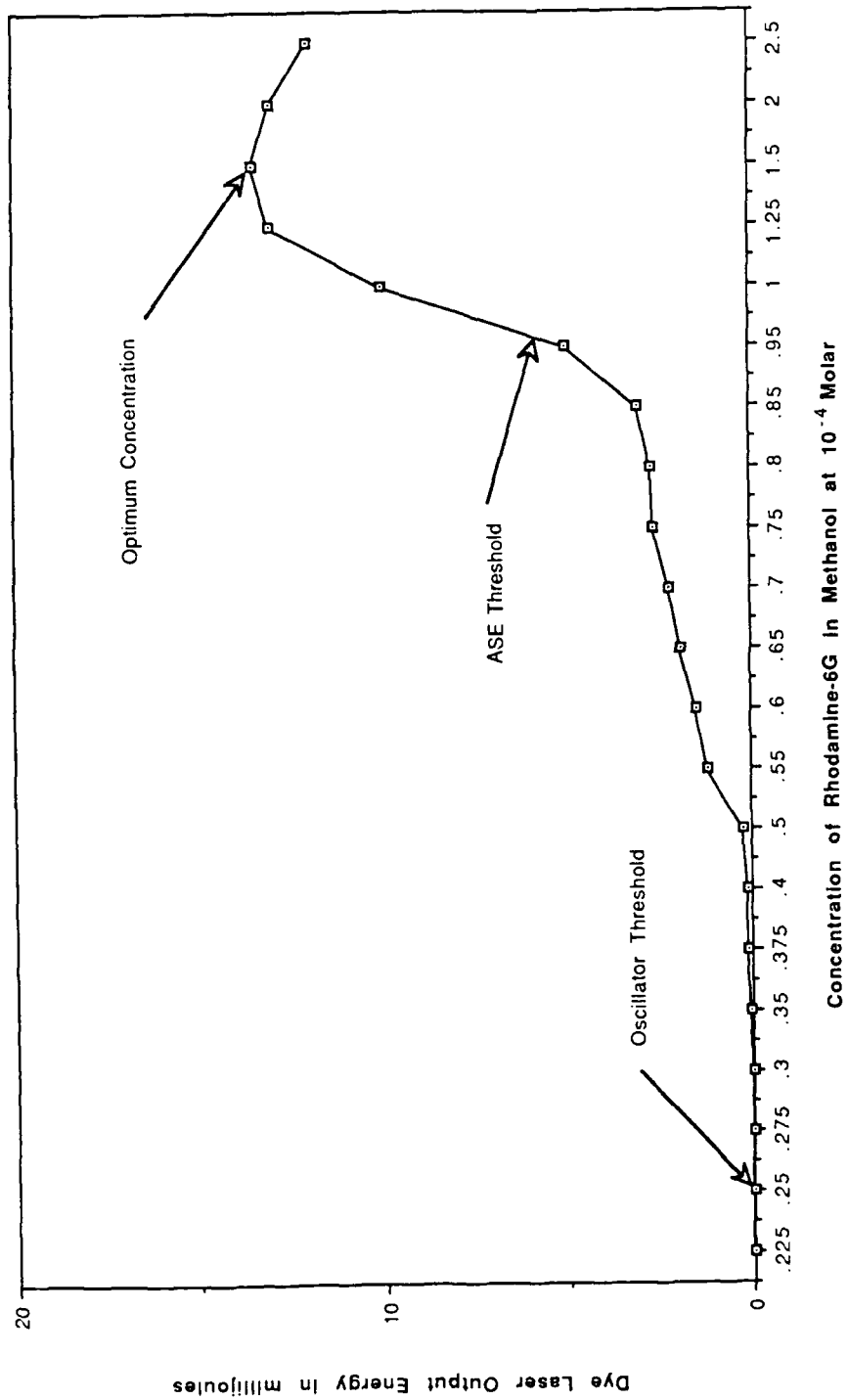


Figure 6. Dye laser output energy vs dye concentration.

cell, the more ASE will occur. Thus, if the oscillator could utilize the concentration that was found to be optimum,  $1.5 \times 10^{-4}$  Molar, and the amplifier utilized a concentration of around  $9.5 \times 10^{-5}$  Molar where ASE was not a problem, then perhaps the ASE would not be as big of a problem in the HyperDYE-300 as it proved to be.

It should also be mentioned that the way the HyperDYE-300 was designed, a serious bubble problem exists with the amplifier dye cell. The dye flows from the reservoir, through a bubble filter, and then upwardly and transverse to the laser cavity through the oscillator. The dye then flows from the top of the oscillator cell to the top of the amplifier cell via 1/4 inch teflon tubing. The dye then flows downward through the amplifier cell, past the knife-edge, and then back to the dye reservoir via more 1/4 inch teflon tubing. Since the dye is flowing downward through the amplifier cell, and due to the fact that buoyancy bubbles tend to rise upward, any bubbles that are passed through the bubble filter are eventually trapped by the opposing forces in the amplifier cell. Also, the knife-edge tends to retard the bubbles from leaving the laser axis. When these bubbles are trapped on the laser axis, the change in refractive index disperses the laser photons and very few, if any, of them make it out of the amplifier cell. It was found that the simplest way to correct this problem was to reverse the dye flow direction so it would flow upward, thus washing the bubbles upward and out of the amplifier cell. This was done easily by interchanging the dye flow leads to the amplifier cell.

#### IV. DATA

Once the dye laser was aligned and optimized, its characteristics were measured. With the dye laser utilizing a  $1.5 \times 10^{-4}$  Molar solution of R-6G in methanol, it was found to be tuneable from 545 nm to 590 nm (see Fig. 7). This is a typical tuning curve for Nd:YAG pumped R-6G. Figure 8 is the optical efficiency of the dye laser (dye laser output divided by doubled Nd:YAG output) versus wavelength. This graph shows that at a lasing wavelength of 565 nm, there was an efficiency of more than 50 percent. The graph also shows that there is approximately a 20 nm range where an efficiency of greater than 30 percent exists. Figure 9 is the energy of the dye laser output versus the energy of the Nd:YAG output. As the pump source was increased in energy, the dye laser output increased linearly. However, from this graph it can also be observed that as the output energy of the dye laser increases it begins to increase slower no matter how much pump energy is being utilized. This can be seen more clearly in Figure 10, which is the slope efficiency of the dye laser. This graph depicts an increase in energy of the dye laser output versus an increase in energy of the Nd:YAG output. It is obvious from this graph that the output energy of the dye laser is not linear with respect to the output energy of the pump beam. In other words, there is most definitely a maximum energy that can be achieved from pumping the HyperDYE-300 with doubled Nd:YAG laser output. This maximum energy was found to be about 35 mJ.

Temporal and spatial profiles of the dye laser output were obtained. The temporal output was observed by utilizing a fast photodiode and a Tektronics storage oscilloscope. In most cases with pulsed laser-pumped dye lasers, the output of the dye laser tends to "track" the pump laser beam. In other words, the temporal profile of the dye laser output should appear very similar to that of the pump source. Figure 11 is the temporal profile of the Nd:YAG laser output. At full-width half-maximum (FWHM) the pulse was about 12 nsec long. Also, from the temporal profile of the Nd:YAG it can be seen that the laser pulse was single mode. The jagged parts of the trace hint that a degenerate mode might have been trying to lase. Figure 12 shows the temporal profile of the dye laser output. The pulse is about 7 nsec wide at FWHM and is single mode. However, like the pump profile, the jagged parts of the trace appear which is due to the dye laser pulse following the pump pulse. It is not due to any degenerate modes in the dye laser, because the dye laser oscillator was designed in such a way that suppresses degenerate mode lasing. In many cases, when the Nd:YAG output was a smoother single mode output, so was the dye laser output. Figure 13 is a temporal profile of the dye laser output that is about 7 nsec wide at FWHM and is perfectly smooth - most definitely single mode.

Spatial profiles of the dye laser output were taken utilizing a frame grabber and beam analysis hardware and software by Big Sky. Figure 14 is a 3-D representation of the laser output near lasing threshold. This is evidence that the laser beam was lasing in the TEM<sub>00</sub> mode. Also, the 3-D plot is typical of a Gaussian laser output, which is representative of good beam quality. Figure 15 is a 3-D representation of the dye laser output at maximum lasing energy, and is also TEM<sub>00</sub> mode. Again, the plot is Gaussian and representative of good beam quality. The number of spatial modes did



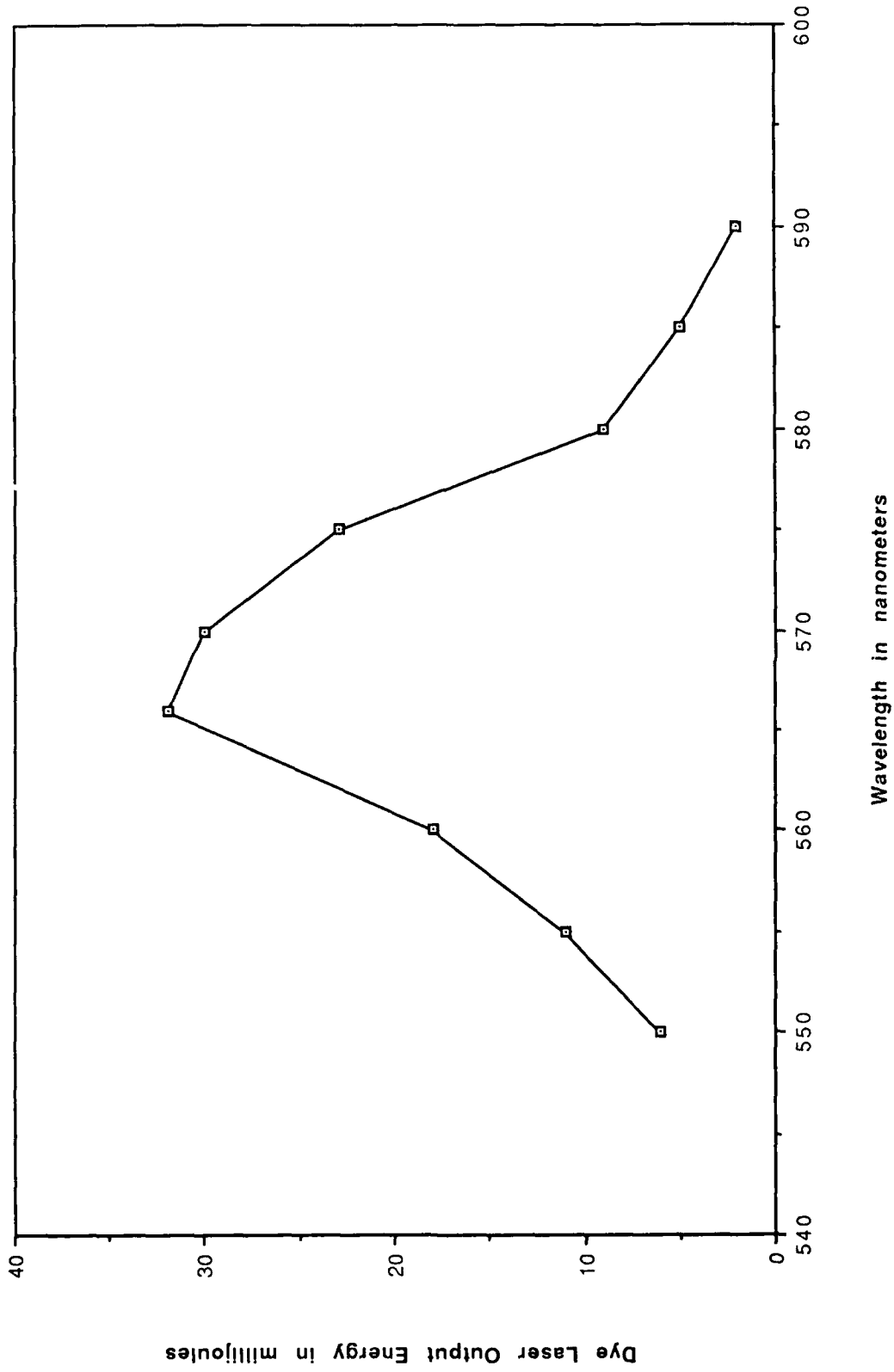


Figure 7. Dye laser output energy vs wavelength.

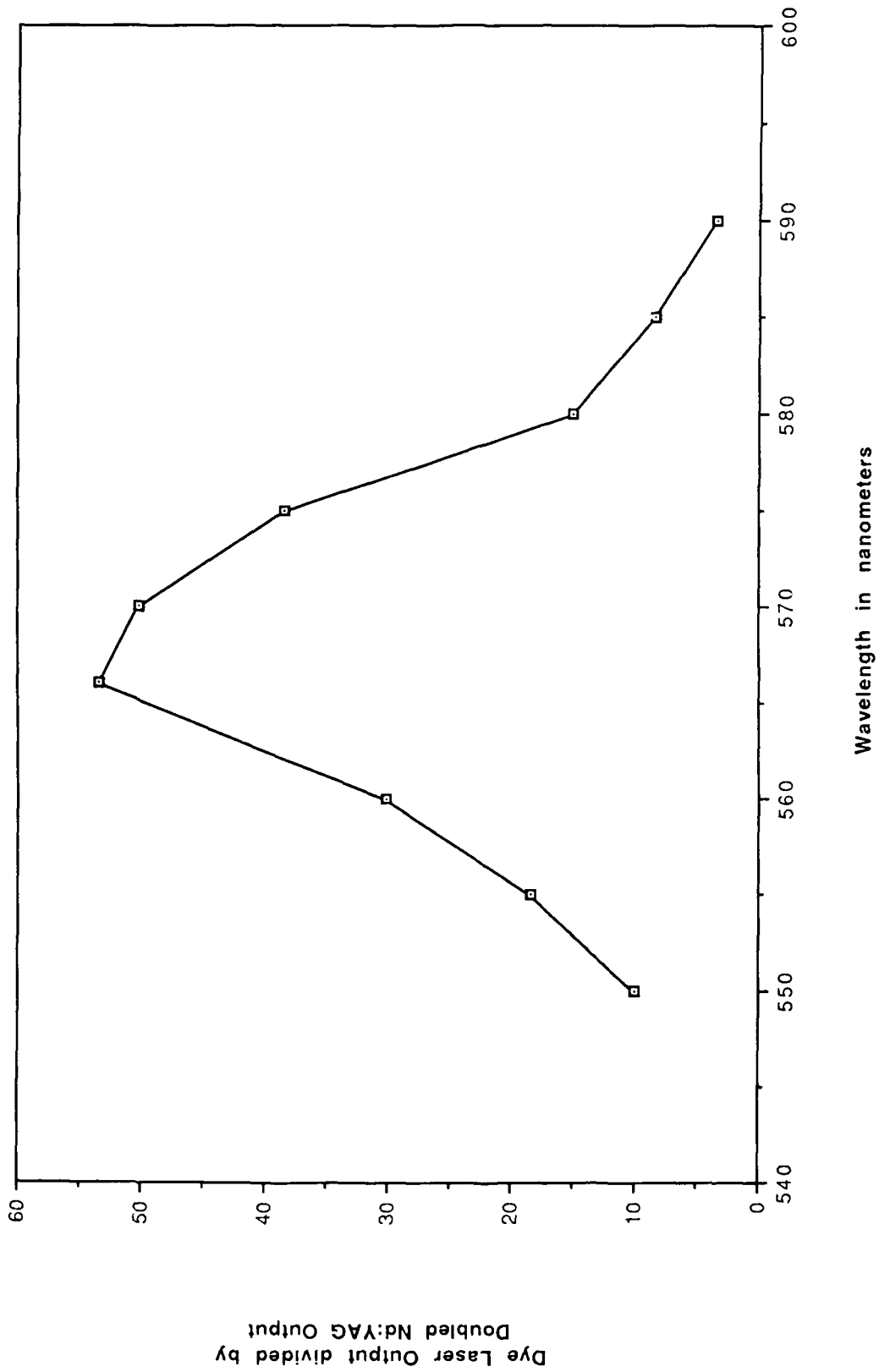


Figure 8. Optical efficiency vs wavelength.

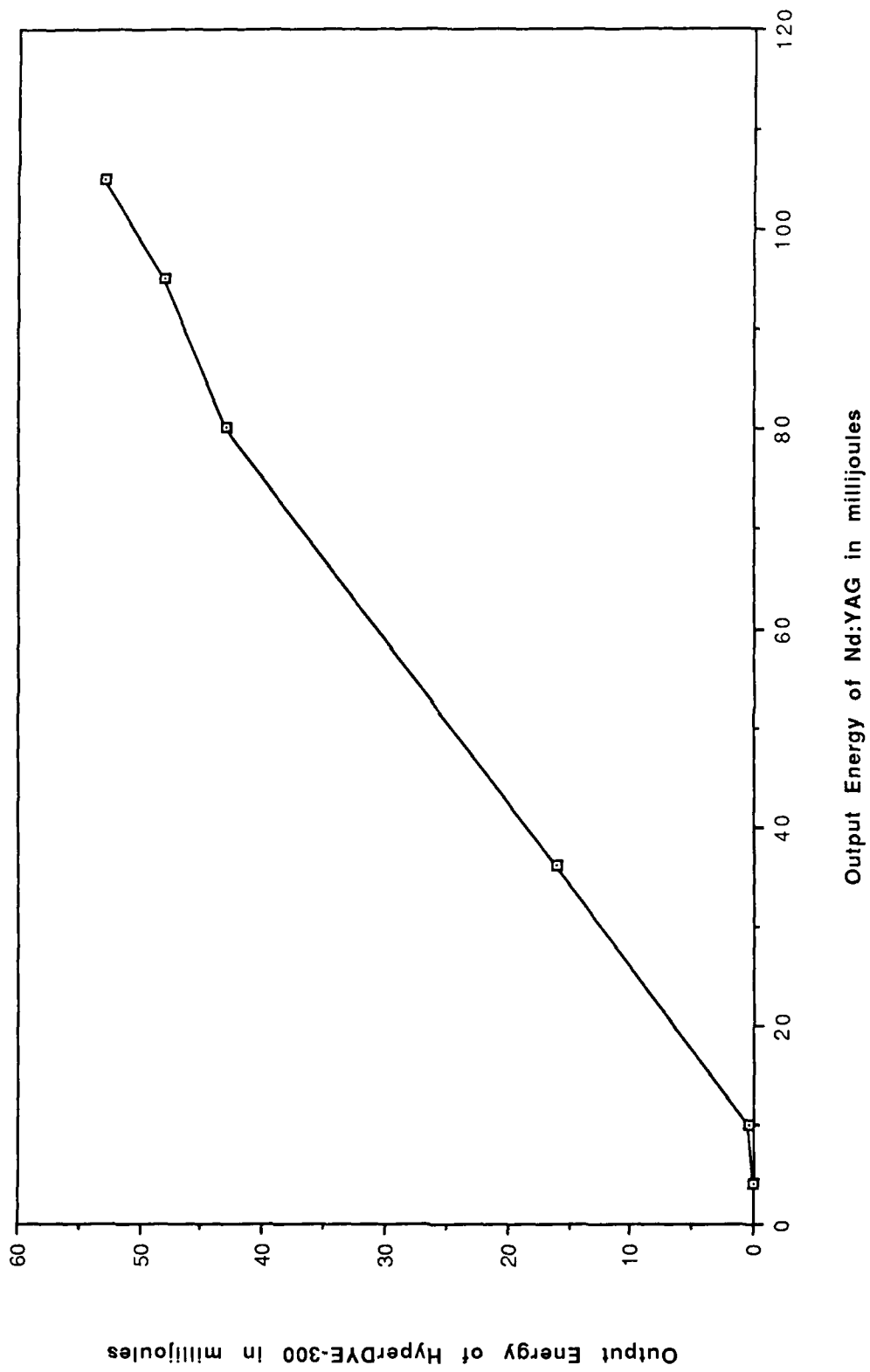
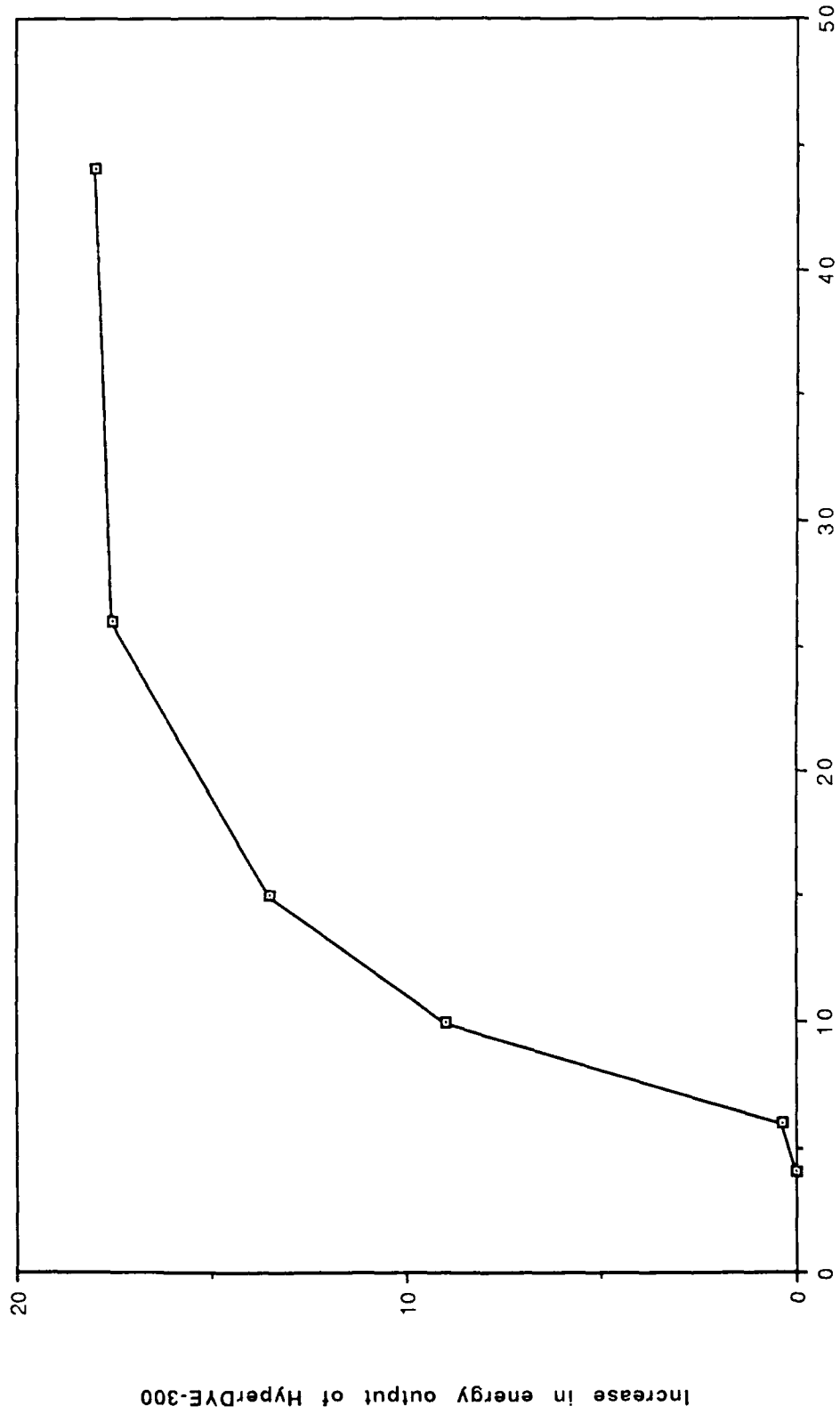


Figure 9. Energy of HyperDYE-300 output vs energy of Nd:YAG output.



Increase in energy output of Nd:YAG

Figure 10. Slope efficiency of Hyper DYE-300.

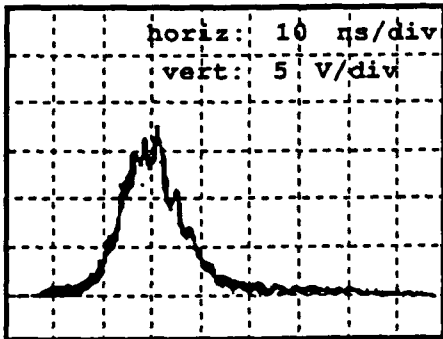


Figure 11. Temporal profile of Nd:YAG output.

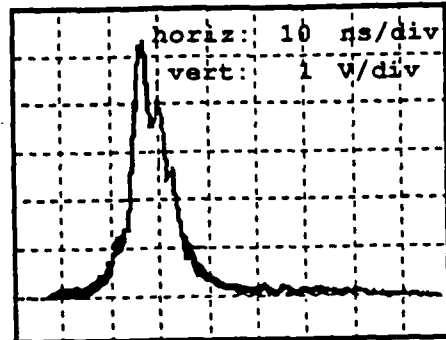


Figure 12. Temporal profile of HyperDYE-300.

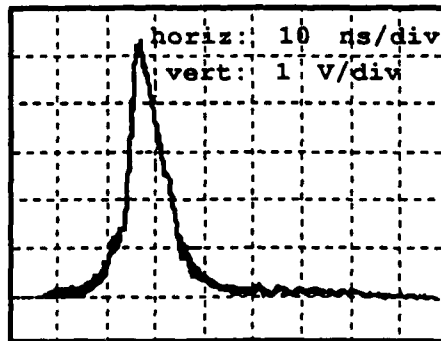


Figure 13. Single mode temporal profile of HyperDYE-300.

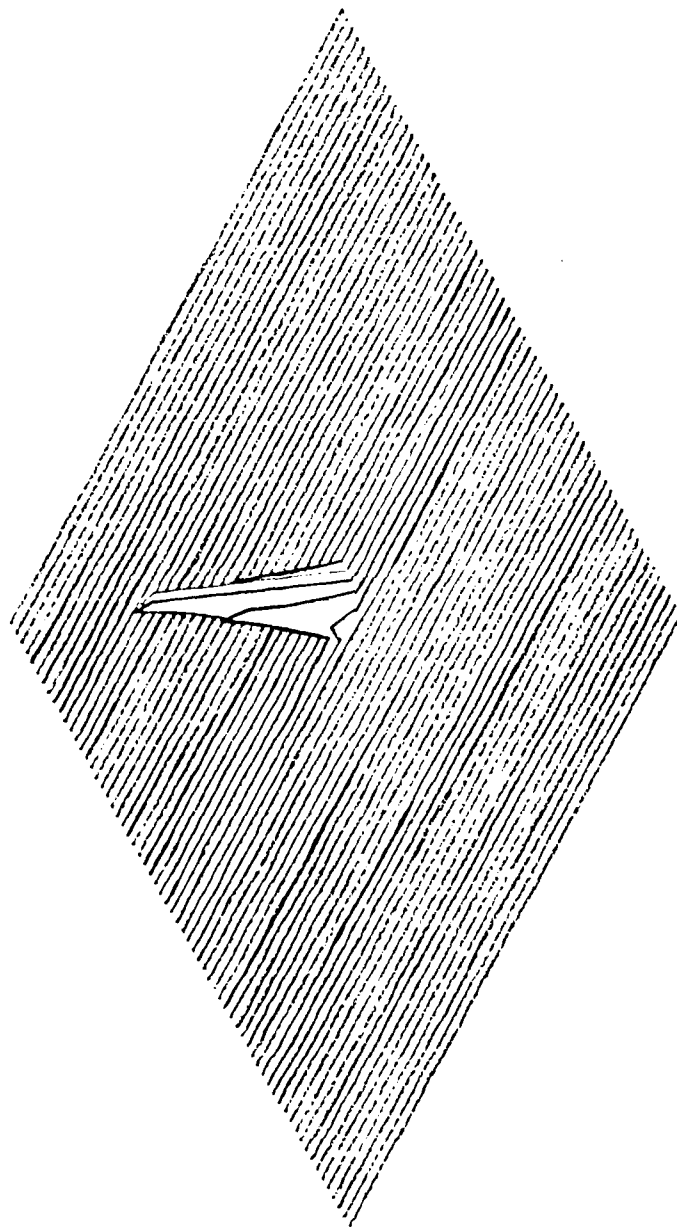


Figure 14. Spatial profile of low energy dye laser pulse.

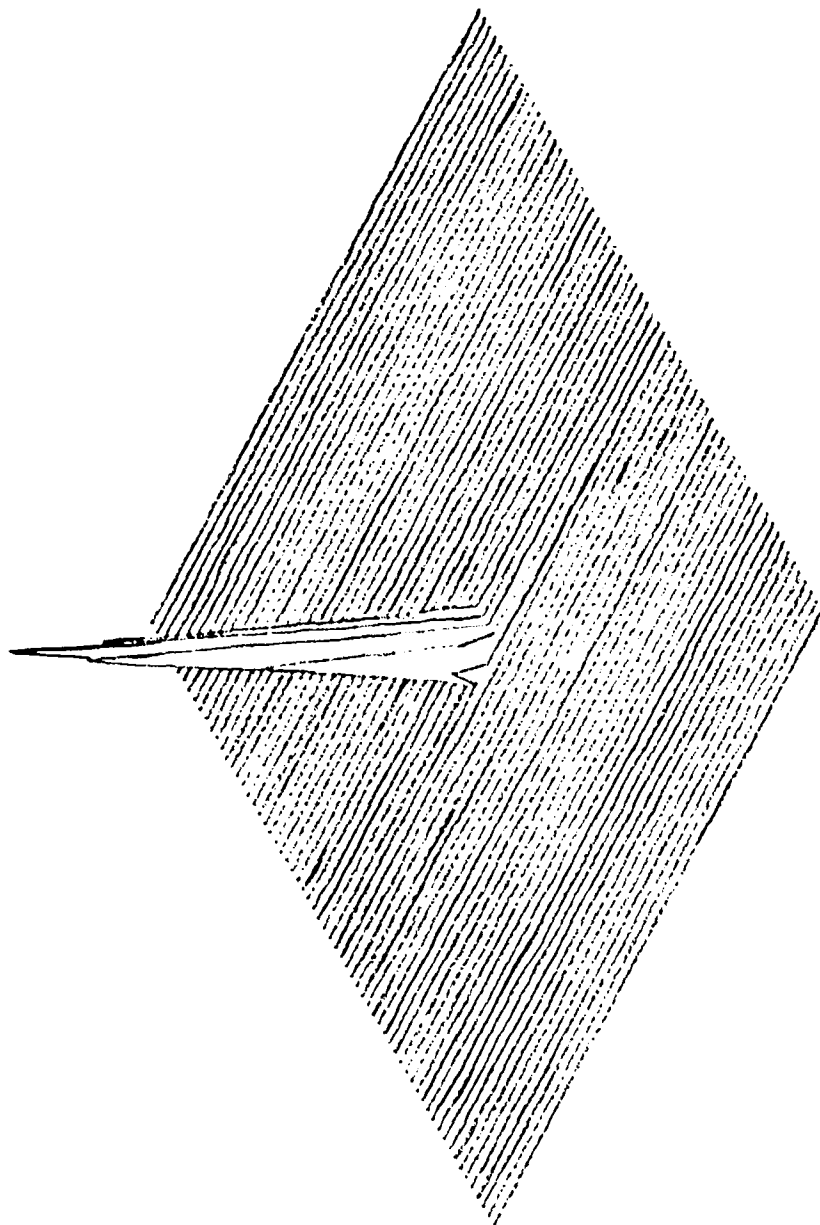


Figure 15. Spatial profile of high energy dye laser pulse.

not change due to an increase in pump energy. Hence, even though there was high gain and large amounts of ASE, no parasitic modes were observed to lase. This stable beam quality is somewhat typical of HMPGI type oscillators.

The half angle beam divergence was measured utilizing the Big Sky hardware, software, and a long focal length positive lens. Table 1 is the data recorded from this experiment. Pulses at four different laser output energies were observed. The x and y-axis focal spot diameters, the effective focal spot diameter at  $1/e^2$  energy, and the divergence were measured. The four energies ranged from just above threshold to maximum output. The half angle beam divergence averaged over the total range of laser output energies was found to be about .3 milliradians. This is better than the manufacturer claim of .5 milliradians by more than 25 percent.

Since ASE had proven to be such a problem during the optimization of the HyperDYE-300, a measurement of ASE photons versus laser photons was made. This measurement of spectral purity<sup>2</sup> was made utilizing a monochromator which was then dispersed by the grating in the monochromator and passed into the photomultiplier tube via another narrow slit. By tuning the grating of the monochromator, relative laser output at discrete wavelengths could be monitored on the oscilloscope. The laser was tuned to a wavelength of 557.39 nm where most of the output photons were observed. However, the ASE background was so bright that it was observed as far as ten nanometers on either side of the laser peak. Figure 16 shows the spectral purity of the oscillator output. Note that the narrow and high peak is the laser output and the "wings" of the curve depict the ASE background. Figure 17 is a closer view of this data. From this curve the actual spectral purity can be approximated by integrating the area under the wings of the curve (the ASE background), dividing it by the area under the remaining portion of the curve (the laser radiation), and then subtracting this value from unity. This was done by implementing a graphics integration program in BASIC and a graphics program on a Macintosh II computer. The spectral purity calculated from this graph was approximately 90 percent. The manufacturer's claim is of a spectral purity of 99.99 percent; therefore, there is about a 9 percent difference in the experimental data and the manufacturer's claim. Figure 18 is the spectral purity of the oscillator-amplifier. From this graph it is obvious that the spectral purity of the oscillator-amplifier is worse than that of the oscillator. This is to be expected since there was such an ASE problem observed with the amplifier. The manufacturer's claim is of a spectral purity of better than 99 percent. The experimental value was on the order of 86 percent. The percent difference between the manufacturer's claim and the experimental data is slightly more than 13 percent.

In order to make the above calculations it was necessary to measure the linewidth of the laser in order to know which parts of the curves in Figures 16 through 18 were laser radiation and which were not. The linewidth of the dye laser was measured from the Fabry-Perot ring pattern in Figure 5. By dividing the width of the second ring by the distance between the first and third ring and then multiplying by the Free Spectral Range (FSR) of the Fabry-Perot etalon, a very good approximation of the linewidth was achieved. The FSR of the etalon was approximately 7.49 GHz. The linewidth of the dye laser output was then measured to be slightly more than 1.69 GHz. The theoretical linewidth can be calculated by utilizing the linewidth equation for HMPGI type laser oscillators.<sup>3,4</sup>



TABLE 1. Beam Divergence Data

LASER PULSE #	#1	#2	#3	#4	AVE.
TOTAL POWER (RELATIVE IN mW)	13890	25070	34750	36750	N/A
EFFECTIVE BEAM DIAMETER AT 1/e <sup>2</sup> (mm)	.5	.5	.5	.6	.5
BEAM DIAMETER ON Y-AXIS (mm)	.5	.6	.7	.6	.6
BEAM DIAMETER ON X-AXIS (mm)	.5	.5	.5	.6	.5
DIVERGENCE (in mrad)	.3	.3	.3	.3	.3

Note: Data taken in order to determine spot size and divergence of Hyper DYE-300 dye laser beam (data was taken with a frame-grabber, camera, and respective software).

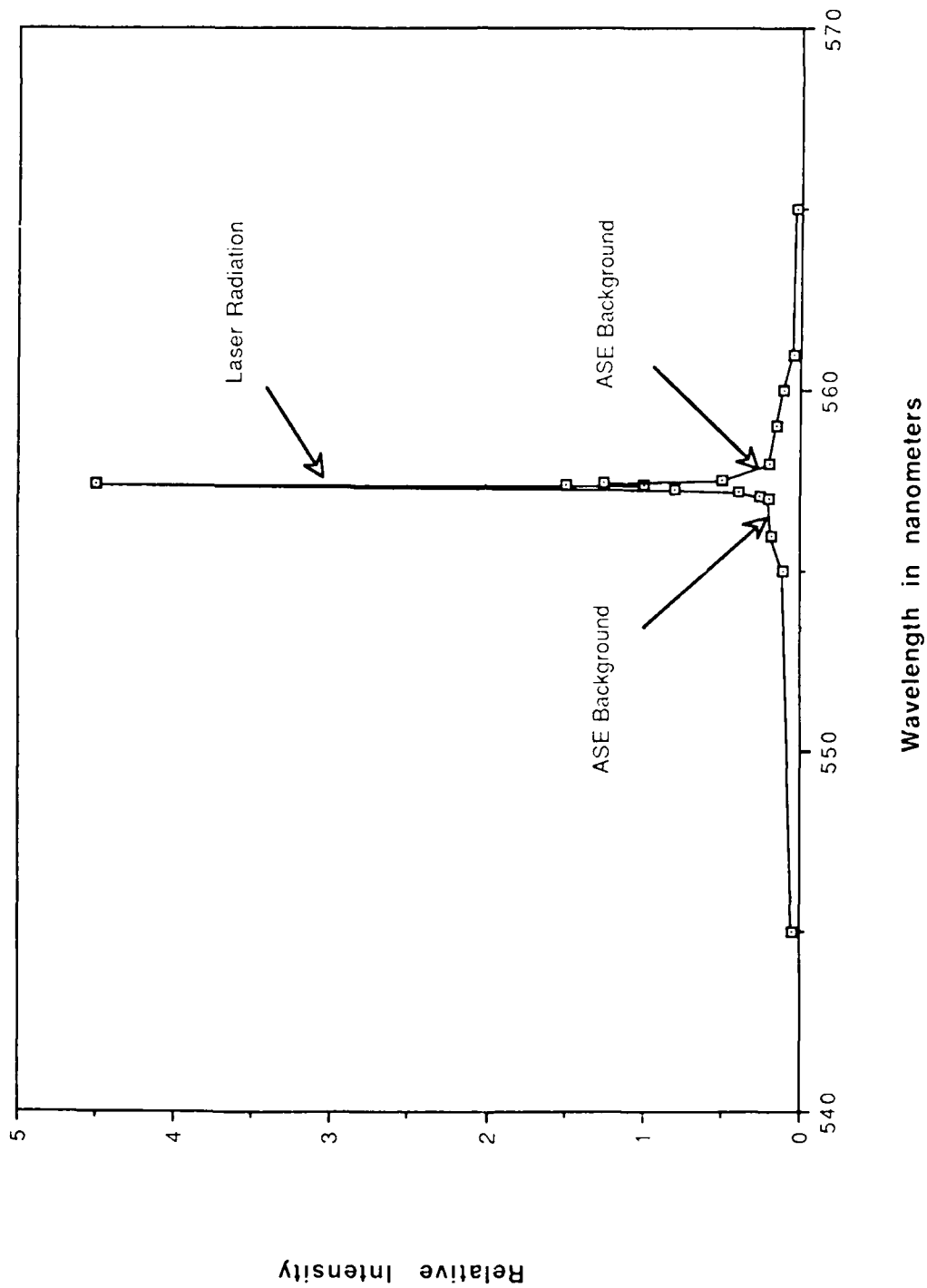


Figure 16. Spectral purity of HyperDYE-300 oscillator.

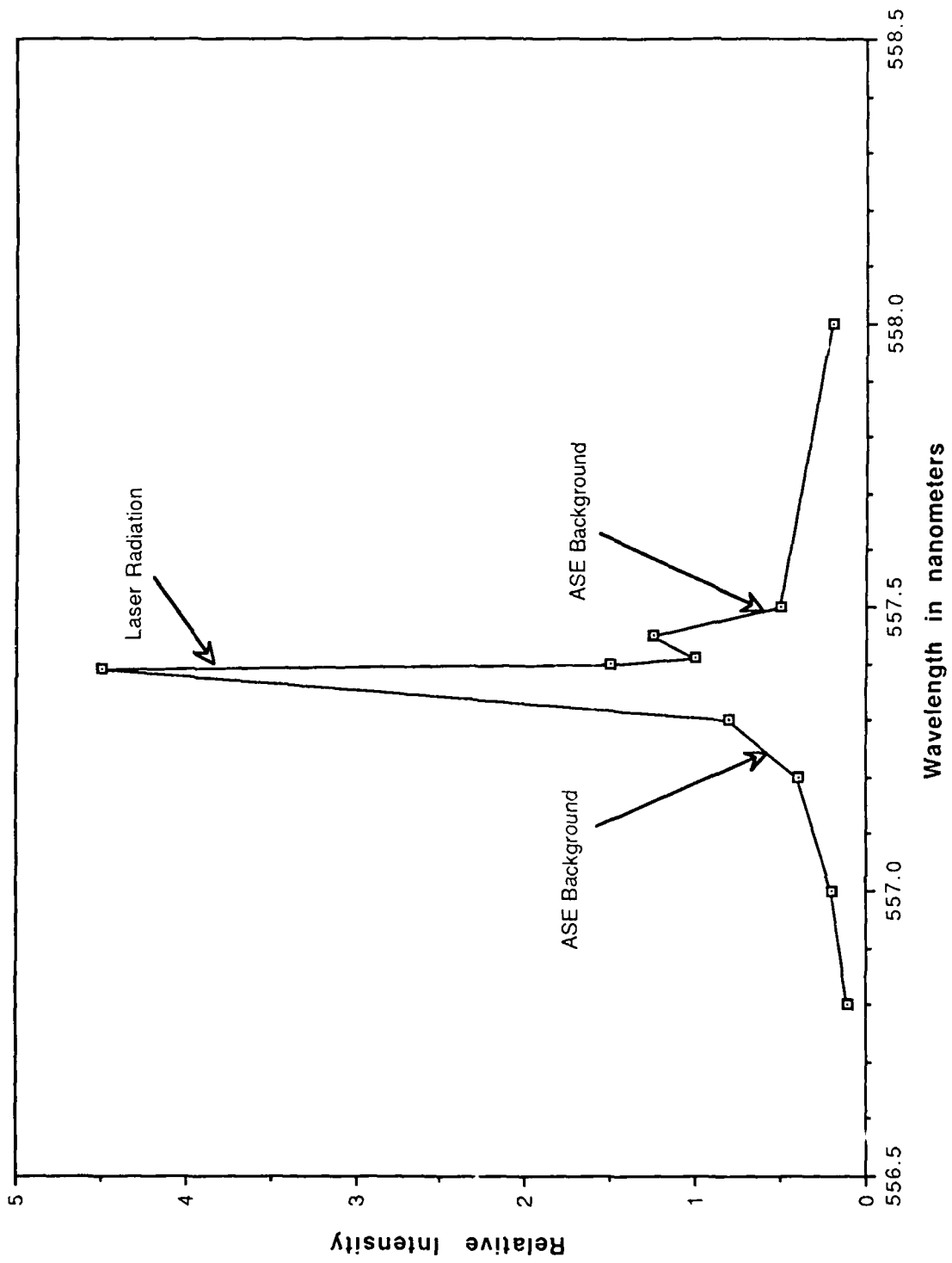


Figure 17. Spectral purity of HyperDYE-300 oscillator.

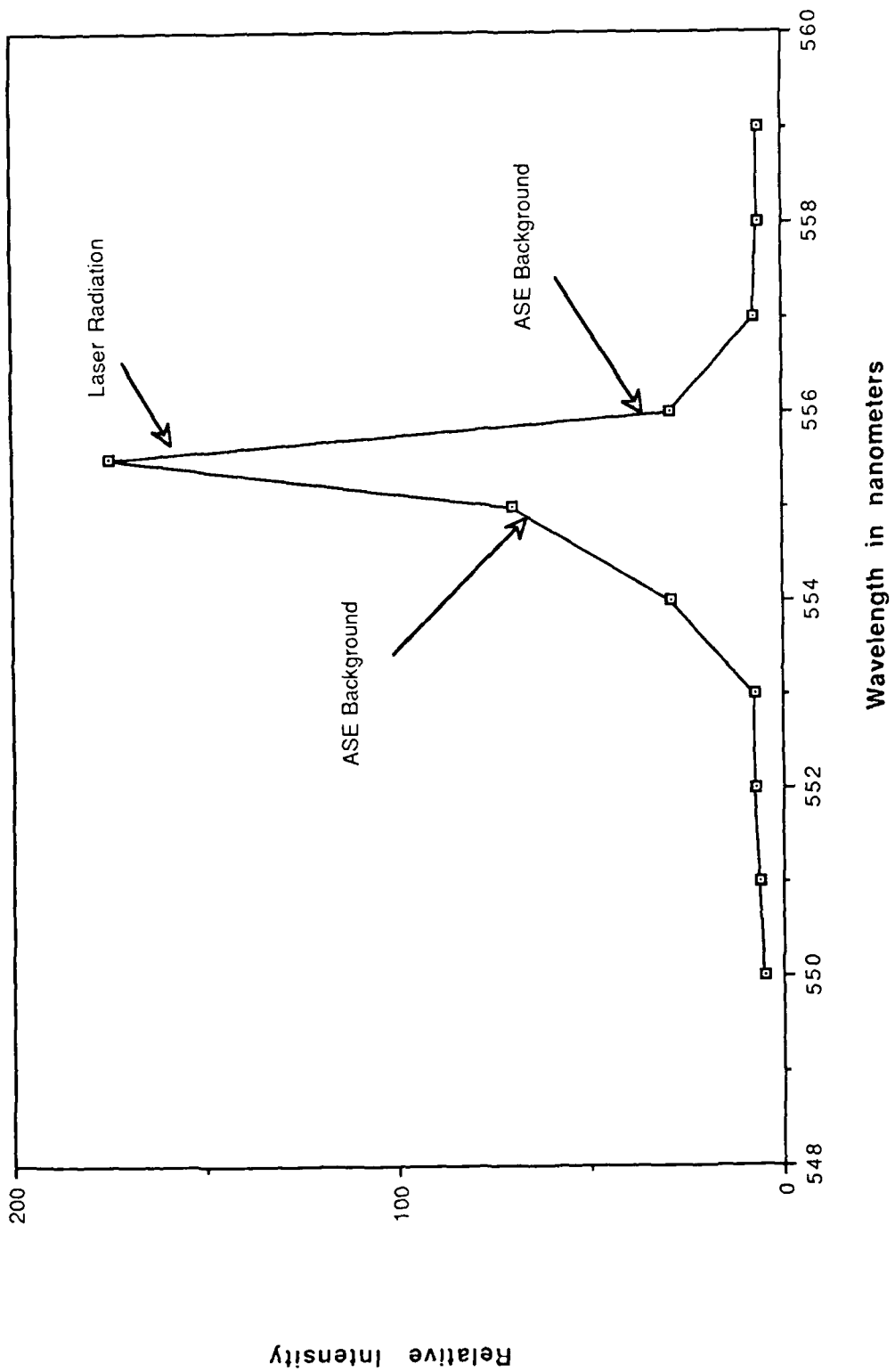


Figure 18. Spectral purity of HyperDYE-300 oscillator-amplifier.

$$\Delta\lambda = (\Delta\theta/R) \left[ \prod_{m=1}^r k_m (\partial\theta/\partial\lambda)_G + 2 \sum_{m=1}^r (\pm 1) \left( \prod_{j=1}^m k_j \right) \tan \psi_{1,m} (dn/d\lambda) \right]^{-1}$$

Where  $\Delta\theta$  is the experimentally determined beam divergence,  $\partial\theta/\partial\lambda$  is the dispersion of the grating,  $dn/d$  is a characteristic of the material from which the prisms are made,  $R$  is the number of intracavity passes, and the term  $k$  corresponds to the expansion due to each prism. The calculated value for the linewidth of the HyperDYE-300 oscillator was determined to be approximately 1.31 GHz. This is slightly better than the actual observed linewidth. One possible explanation for the difference between the experimental and calculated values might be that the theoretical calculations obviously do not account for ASE. There is enough ASE that occurs in the oscillator to broaden the linewidth of the dye laser output.

## V. CONCLUSIONS

Using a Nd:YAG pulsed laser to pump the HyperDYE-300 dye laser, optimum dye concentration for R-6G in methanol, output energy versus wavelength, optical efficiency versus wavelength, and slope efficiencies were determined. The dye laser was observed as lasing in only one temporal mode and the spatial profiles of the output suggests TEM<sub>00</sub> mode lasing as well. The divergence and the linewidths of the dye laser output were found to be as good as, if not better, than the manufacturer's claim. However, according to theoretical calculations the linewidth could possibly be slightly better than that observed. The reason the linewidth was not optimum was most likely due to ASE in the dye laser cavity. The ASE versus laser output was measured and was not found to be quite as good as the manufacturer's claim. In order to defeat the ASE, various alignment procedures and dye/solvent concentrations were tried. The dye laser was manufactured with only one dye flow system, so both the amplifier and the oscillator must use the same dye. The dye concentration that was ideal for the oscillator was too concentrated for proper operation of the amplifier, thus creating an amplifier gain media that was nearly saturated with ASE. Ideally, there should be two dye flow systems, one for the oscillator and one for the amplifier. This way the concentration of the oscillator could remain high, while the concentration of the amplifier could be reduced. With the amplifier dye concentration reduced, the gain would also be reduced. Thus, the main problem with the HyperDYE-300 - ASE - might be overcome.

#### REFERENCES

1. Lumonics HyperDYE-300 Series Pulsed Dye Laser Instruction Manual, Lumonics Inc., Ontario, Canada, 1988.
2. McKee, T. J., Lobin, J., and Young, W. A., "Applied Optics, 21," 725 1982.
3. Duarte, F. J., Conrad, R. W., Patterson, S. P., and Russell, S. D., from the Proceedings of the International Conference on Lasers '85, (STS Press, McLean, VA, 1986) pp. 153-157.
4. Duarte, F. J., "Opt. and Quantum Electron. 21" 47, 1989.

DISTRIBUTION

	<u>Copies</u>
U.S. Army Materiel System Analysis Activity ATTN: AMXSU-MP (Herbert Cohen) Aberdeen Proving Ground, MD 21005	1
IIT Research Institute ATTN: GACIAC 10 W. 35th Street Chicago, IL 60616	1
AMSMI-RD	1
AMSMI-RD-DE-LT, Mr. Taylor	50
AMSMI-RD-CS-R	15
AMSMI-RD-CS-T	1
AMSMI-GC-IP, Mr. Bush	1
AMSMI-SI-FO, Mr. Huber	1